Sensitivity-based Predictive Control of a Large-scale Supermarket Refrigeration System ⋆

Christian Sonntag * **Malte Kölling** ** **Sebastian Engell** *

* *Process Dynamics and Operations Group (BCI-DYN), Dept. of Biochemical and Chemical Engineering, Technische Universität Dortmund, 44221 Dortmund, Germany E-mail: {christian.sonntag|sebastian.engell}@bci.tu-dortmund.de.*
** *Hydro Aluminium, 41515 Grevenbroich, Germany E-mail: malte.koelling@hydro.com*

Abstract: Today, many supermarket refrigeration systems are operated by decentralized control systems that often lead to excessive starting and stopping of the compressors which drive the cooling cycle and, consequently, to a large wear of the process equipment. In our previous work, a hierarchical model-predictive control scheme was proposed for supermarket refrigeration systems that overcomes this drawback. In this scheme, simple low-level temperature controllers are employed, and the high-level optimization task is the optimal adjustment of the parameters of these controllers. While this approach yields a good control performance, it is computationally too expensive for larger systems. In this paper, a more efficient approach is presented that is based on an approximation of the system dynamics using simple models that are computed from system sensitivities around simulated reference trajectories. The application of the new approach to a large hybrid model proves the real-time capabilities of the new technique.

Keywords: Predictive control, process control, supermarket refrigeration systems, discretely controlled continuous systems, hybrid systems.

1. INTRODUCTION

In supermarket refrigeration systems, a rack of compressors feeds liquid refrigerant to several open display cases that are used to cool edible goods. These systems exhibit both, discrete and continuous dynamics, and are thus hybrid systems: The control inputs (valves and compressors) can only be switched discretely, and the nonlinear continuous dynamics changes due to switching of the discrete inputs. Today, supermarket refrigeration systems are often controlled using decentralized schemes in which each display case is equipped with independent simple control loops (Larsen et al., 2005). Since this approach often causes a severe reduction of the efficiency of the process and of the lifespan of the equipment (see e.g. Wisniewski and Larsen (2008)), the suitability of advanced model-predictive schemes for the control of supermarket refrigeration systems has been investigated in previous work to overcome these problems.

In Larsen et al. (2005), the hybrid MPC approach from Bemporad and Morari (1999) is applied to a piecewise affine approximation of the nonlinear hybrid model of a supermarket refrigeration system that is also considered in this paper. Although this approach succeeds in keeping most process variables within pre-specified bounds, the frequency of the compressor switching is high due to the inaccuracy of the linear approximations of the nonlinear dynamics. In Sarabia et al. (2009), a nonlinear MPC scheme is proposed in which the cost function is evaluated by simulation of a nonlinear model. This approach is capable of keeping all process variables within the bounds, but the solution of complex NLP problems with many decision variables in each iteration leads to a large computational effort. In Sonntag et al. (2007, 2008), a hierarchical NMPC approach for supermarket refrigeration systems is presented. Here, the switching of the valves of the display cases is not optimized directly, but simple low-level controllers are employed that regulate the temperatures in the display cases with a high sampling frequency. The parameters of these controllers are adjusted by a high-level NMPC optimizer that operates on a longer time horizon, thus leaving more computation time for the NLP step in every NMPC iteration. Instead of considering a (complex) MINLP problem in each iteration, the discrete search is performed by solving a sequence of continuous optimization problems with an increasing number of switches, and the search is stopped as soon as a policy is found that meets the specification. This reflects the main control goal, the minimization of the number of switches of the compressors.

While the NLP-based approaches that are described above yield a good control performance, they cannot currently be applied to larger systems in real time due to the prohibitively large computational effort. To overcome this problem, this paper presents a new and computationally

⋆ The authors gratefully acknowledge the financial support by the EU-funded Network of Excellence HYCON, contract number FP6-IST- 511368.

more efficient hierarchical model-predictive control approach for supermarket refrigeration systems. As in Sonntag et al. (2007, 2008), the switching of the valves of the display cases is not optimized directly, but simple low-level controllers are employed that regulate the temperatures in the display cases. The high-level approach presented in this paper differs from the previous version in two respects: the compressors are not switched by the high-level controller anymore since the corresponding control goal for the suction pressure is merely safety-related, and it is not necessary to achieve optimality in this part of the system. A simple discrete low-level controller is employed instead. Furthermore, the optimization approach of the high-level controller is significantly different. It is based on the observation that the considered supermarket refrigeration system belongs to an important subclass of hybrid systems, the *Discretely Controlled Continuous Systems* (DCCS). These systems have been investigated in academia for many years, see e.g. Matveev and Savkin (2000); Dankowicz and Piiroinen (2002); Schild and Lunze (2008). The property of DCCS that is exploited in this paper is that simple yet accurate finite-dimensional models of the system behavior (the so-called *embedded maps* of the system) can be approximated linearly around simulated reference trajectories based on the sensitivities of the continuous subsystems. These low-dimensional embedded maps are then used as linear constraints in the optimizing high-level control system, and the complex dynamic optimization problem can be recast as a sequence of algebraic optimization problems. In combination with a decomposition of the large-scale supermarket system into (virtually) independent subcomponents which are approximated separately, this new approach allows for a very efficient computation of optimal switching times which enables the real-time control even of large-scale supermarket systems.

2. THE SUPERMARKET REFRIGERATION SYSTEM

Fig. 1 shows a schematic representation of a supermarket refrigeration system. It consists of five major parts: a liquid manifold, several display cases, a compressor rack, a suction manifold, and a condenser. Liquid refrigerant is supplied to the display cases from the liquid manifold through inlet valves (see Fig. 2). Within each display case, cold air circulates and forms an air curtain in front of the edible goods. Thermal energy is transferred from the goods to the air curtain ($\dot{Q}_{goods-air}$) and, since the temperature of the surrounding air is larger than that of the air curtain, the curtain also absorbs heat from the surroundings ($\dot{Q}_{airload}$). The absorbed thermal energy is transported to the evaporator ($\dot{Q}_{air-wall}$) in which the refrigerant evaporates and thus takes on the thermal energy ($\dot{Q}_e$). The vapor accumulates in the suction manifold and is fed to the condenser via the compressors which increase the pressure of the refrigerant vapor. Since the evaporation temperature of the refrigerant increases with the pressure, the energy from the display cases can be removed in the condenser at room temperature. Finally, the liquefied refrigerant is fed back to the display cases.

The hybrid model of the supermarket refrigeration system used in this work was proposed in Larsen et al. (2007). It may contain an arbitrary number of display cases n_{dc}. The state of each display case $i \in \{1, \dots, n_{dc}\}$ is described by four differential state variables: the temperature of the goods ($T_{g,i}$), the temperature of the evaporator wall ($T_{w,i}$), the temperature of the air inside the case ($T_{air,i}$), and the mass of liquid refrigerant within the evaporator of the display case ($m_{ref,i}$). Thus, the vector of continuous state variables of the i-th display case is given by $\mathbf{x}_{dc,i} = [T_{g,i}, T_{w,i}, T_{air,i}, m_{ref,i}]^T$. Since the dynamics of the condenser unit is not modeled, the overall continuous state vector of the model can be written as $\mathbf{x} = [\mathbf{x}_{dc,1}^T, \dots, \mathbf{x}_{dc,n_{dc}}^T, P_{suc}]^T$, where P_{suc} is the pressure in the suction manifold. Each display case is equipped with an expansion valve for the refrigerant, and the discrete input vector is given by $\mathbf{v} = [v_1, \dots, v_{n_{dc}}, v_c]^T$. Here, $v_1, \dots, v_{n_{dc}} \in \{1, 0\}$ are binary variables representing the state of the inlet valves (open/closed), and $v_c \in \Xi_c$ (given in %) determines the relative capacity of the compressors that are currently running within the compressor rack [1]. The set Ξ_c contains all discrete capacity levels that can be realized by switching the compressors on or off. In this paper, a system with six compressors of equal capacity is investigated. For this system, Ξ_c is defined as:

$$\Xi_c := \{0\%, 16.7\%, 33.3\%, 50\%, 66.7\%, 83.3\%, 100\%\}. \quad (1)$$

[1] Thus, the values 0% (100%) always indicate that all compressors are off (on), independently of the number of compressors.

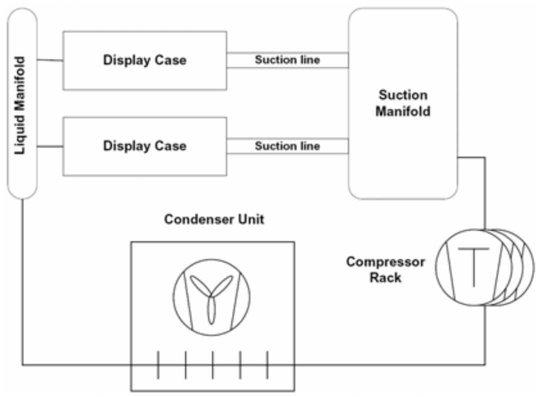

Fig. 1. A simplified scheme of a supermarket refrigeration system with two display cases.

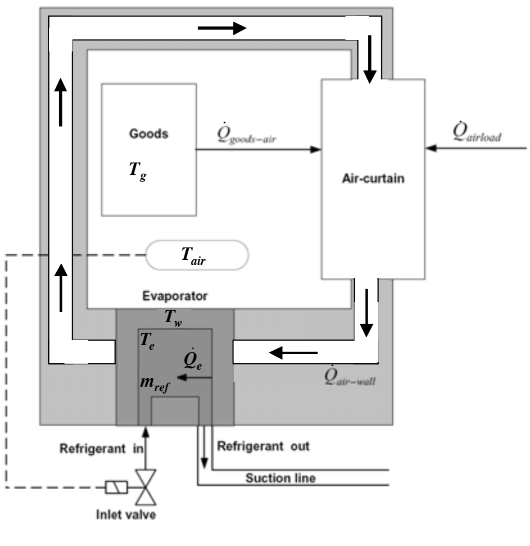

Fig. 2. Cross section of a display case.

The continuous dynamics is modeled by a lumped-parameter ODE system [2] under the assumption that all display cases are of equal design. Each display case exhibits two different continuous dynamics, depending on the setting of the corresponding expansion valve, i.e.

$$\frac{d\mathbf{x}_{dc,i}}{dt} = \begin{cases} \mathbf{f}_{i,vo}(\mathbf{x}_{dc,i}) \text{ if } v_i = 1, \text{ (a)} \\ \mathbf{f}_{i,vc}(\mathbf{x}_{dc,i}) \text{ if } v_i = 0. \text{ (b)} \end{cases} \quad (2)$$

The vector functions $\mathbf{f}_{i,vo}$ and $\mathbf{f}_{i,vc}$ only differ in the dynamic equation that determines the mass of refrigerant in the evaporator of a display case $m_{ref,i}$ according to

$$\frac{dm_{ref,i}}{dt} = \begin{cases} \dfrac{m_{ref,max} - m_{ref,i}}{\tau_{fill}} & \text{if } v_i = 1, \text{ (a)} \\ -\dfrac{\dot{Q}_{e,i}}{\Delta h_{lg}} & \text{if } v_i = 0. \text{ (b)} \end{cases} \quad (3)$$

Here, the maximum mass of refrigerant each display case can accommodate is represented by $m_{ref,max}$, $\dot{Q}_{e,i}$ is defined in Eq. 9, the specific enthaply of evaporation of the remaining liquefied refrigerant in the evaporator is given by Δh_{lg}, and τ_{fill} is a time constant. The display case is filled with refrigerant as long as the inlet valve is open (Eq. 3.a), and after the inlet valve has been closed, the remaining refrigerant evaporates according to Eq. 3.b. The temperature dynamics within the i-th display case does not change with the valve setting and is given by:

$$\frac{dT_{g,i}}{dt} = -\frac{\dot{Q}_{goods-air,i}}{m_{goods} \cdot cp_{goods}}, \quad (4)$$

$$\frac{dT_{w,i}}{dt} = \frac{\dot{Q}_{air-wall,i} - \dot{Q}_{e,i}}{m_{wall} \cdot cp_{wall}}, \quad (5)$$

$$\frac{dT_{air,i}}{dt} = \frac{\dot{Q}_{goods-air,i} + \dot{Q}_{airload} - \dot{Q}_{air-wall,i}}{m_{air} \cdot cp_{air}}, \quad (6)$$

with

$$\dot{Q}_{goods-air,i} = UA_{goods-air} \cdot (T_{g,i} - T_{air,i}), \quad (7)$$

$$\dot{Q}_{air-wall,i} = UA_{air-wall} \cdot (T_{air,i} - T_{w,i}), \quad (8)$$

$$\dot{Q}_{e,i} = UA_{wall-ref}(m_{ref,i}) \cdot (T_{w,i} - T_e(P_{suc})), \quad (9)$$

$$UA_{wall-ref}(m_{ref,i}) = UA_{wall-refmax} \cdot \frac{m_{ref,i}}{m_{ref,max}}. \quad (10)$$

Here, m_{goods}, m_{wall}, m_{air}, cp_{goods}, cp_{wall}, cp_{air}, $UA_{goods-air}$, $UA_{air-wall}$, and $UA_{wall-refmax}$ are constant model parameters, and T_e is the evaporation temperature of the refrigerant which is a nonlinear function of P_{suc}. The dynamics of the suction pressure is given by

$$\frac{dP_{suc}}{dt} = \frac{\dot{m}_{in-suc} + \dot{m}_{ref-const} - \dot{V}_c \cdot \rho_{suc}}{V_{suc} \cdot \frac{d\rho_{suc}}{dP_{suc}}}, \quad (11)$$

with

$$\dot{m}_{in-suc} = \sum_{i=1}^{n_{dc}} \frac{\dot{Q}_{e,i}}{\Delta h_{lg}}, \quad \dot{V}_c = \frac{v_c \cdot \eta_{vol} \cdot V_d}{100}. \quad (12)$$

Here, the total mass flow of refrigerant from all display cases into the suction manifold is given by $\dot{m}_{in-suc}$, and $\dot{m}_{ref-const}$ is a measurable external disturbance that represents an additional flow of refrigerant from other unmodeled cooling facilities into the suction manifold. $\dot{V}_c$ is the volume flow from the suction manifold, and ρ_{suc} and $\frac{d\rho_{suc}}{dP_{suc}}$ are nonlinear refrigerant-dependent functions modeling the density of the vapor in the suction manifold and the derivative of ρ_{suc} w.r.t. the suction pressure, and η_{vol} and V_d are constant model parameters.

[2] See also Larsen et al. (2007).

The controlled variables of the system are the pressure inside the suction manifold (P_{suc}) and the temperatures of the air inside the display cases ($T_{air,i}$). As the system never reaches a steady state since the different continuous dynamics of the display cases have distinct equilibrium points, the control goal is not to track setpoints, but to maintain the controlled variables within specified bounds $\underline{T}_{air,i} \leq T_{air,i} \leq \overline{T}_{air,i}$ and $\underline{P}_{suc} \leq P_{suc} \leq \overline{P}_{suc}$.

3. THE CONTROL STRATEGY

A scheme of the hierarchical control strategy is shown in Fig. 3. This strategy is very similar to the hierarchical approach that was presented in Sonntag et al. (2008), with one important difference: while in Sonntag et al. (2008), the parameters of the low-level controllers as well as the settings of the compressors are adapted by the high-level optimizer, the controlled subsystems are separated into two categories in the new approach: The first category consists of subsystems for which the desired control functionality is only safety-related, i.e. the control goal is to keep a process variable within an admissible region, and a quantitative measure of optimality is not necessary. Among the subsystems of the supermarket refrigeration system, the suction manifold and the compressor rack fall into this category and are not considered in the high-level predictive controller. The second category consists of subsystems for which quantitative optimality measures can be defined. In the supermarket system, the display cases belong to this category since here the control goal, the temporal desynchronization of the air temperatures, can be formulated in a quantitative way that is amenable to minimization. This temporal desynchronization ensures that the variations in the suction pressure and, thus, the necessity for compressor switching are minimized.

3.1 The Low-Level Control System

The switching strategy for the valves of display case i is shown in Fig. 4. The valve of the corresponding display case remains closed as long as the air temperature remains below the switching threshold δ_s. After the refrigerant has evaporated, the air temperature starts to rise. Once the air temperature crosses δ_s from below, v_i is opened for a constant period of time t_{v_i}, and the air temperature will decrease again. The time period t_{v_i} is a continuous parameter that is assigned by the high-level controller for

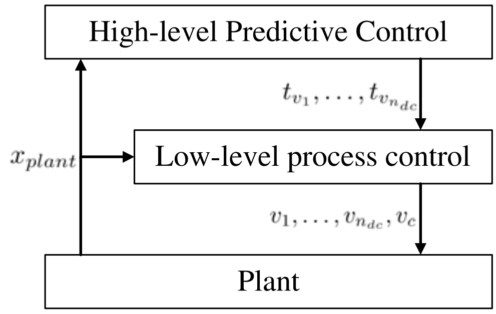

Fig. 3. Scheme of the control strategy.

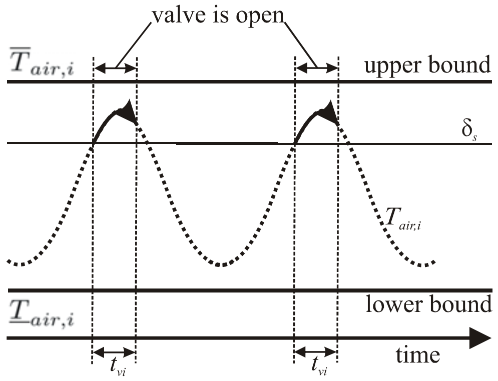

Fig. 4. Switching strategy for the expansion valves for an exemplary evolution of the air temperature of display case i.

each display case ($t_{v_1}, \ldots, t_{v_{n_{dc}}} \in \mathbb{R}^{\geq 0}$ in Fig. 3). The value of δ_s was determined in simulation studies assuming that $T_{air,i}$ will always decrease shortly after the valve v_i is opened (which can be deduced from the continuous model dynamics and parameters).

The low-level pressure controller switches off a compressor if $P_{suc} \leq \underline{P}_{suc}$, and it switches on an additional compressor if $P_{suc} \geq \overline{P}_{suc} - 0.1\ bar$. To avoid excessive switching of the compressors over a short time period, a compressor can only be switched 10 seconds after the previous compressor switch at the earliest. To compensate for fast changes of the external disturbances, an additional controller is employed that monitors the stationary continuous compressor capacity v_{cs} that is needed to keep all process variables within the admissible region over long time periods. From the ODE system, v_{cs} can be computed as:

$$v_{cs} = 100\ \% \cdot \left(\frac{\dot{m}_{in-suc} + \dot{m}_{ref-const}}{\rho_{suc} \cdot \eta_{vol} \cdot V_d} \right). \tag{13}$$

If v_{cs} changes by more than $\delta_c = \frac{1}{2} \cdot \frac{100\ \%}{n_c}$ (n_c is the number of compressors) over a time period of 30 seconds, the controller switches the compressors to the discrete capacity level that is closest to v_{cs}.

3.2 Desynchronizing High-level Control

The high-level controller operates on a moving time horizon. In every iteration, a fixed time interval of t_p seconds is available for the adaptation of the valve opening times $t_{v_1}, \ldots, t_{v_{n_{dc}}}$ of the low-level temperature controllers. The algorithm is based on the assumption that all display cases can be regarded separately, i.e. that the interactions between the display cases are negligible. To confirm this assumption, a sensitivity analysis was performed for the system in which the cross-correlations between the system variables were computed by the solution of the matrix-valued linear sensitivity equation

$$\frac{d\mathbf{S}}{dt} = \frac{\partial \mathbf{f}}{\partial \mathbf{x}} \cdot \mathbf{S}, \quad \mathbf{S}(t_0) = \mathbf{I}. \tag{14}$$

Here, $\frac{\partial \mathbf{f}}{\partial \mathbf{x}}$ is the Jacobian of the dynamic vector equation of the system. It was found that the effect of changes of the state variables $\mathbf{x}_{dc,i}$ of a display case i and the variables $\mathbf{x}_{dc,j}$ of other display cases with $j \neq i$ as well as the effect of changes of the suction pressure P_{suc} on $\mathbf{x}_{dc,i}$ are several orders of magnitude smaller than the effects between the internal variables of the display case in all operating regimes that are relevant for nominal process operation. Thus, the display cases can be considered as independent subsystems for control design purposes.

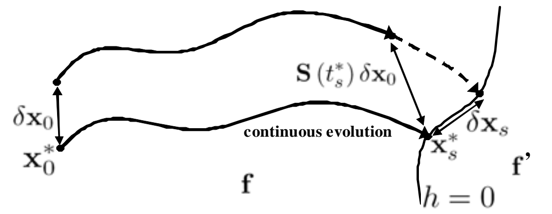

Fig. 5. On the linear approximation of the embedded map.

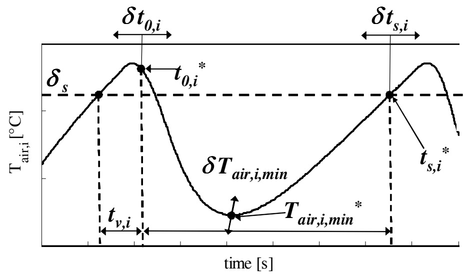

Fig. 6. Application of the approximation procedure to a single display case.

The desynchronization algorithm is based on the computation of an abstract algebraic model (an embedded map) for each display case which is locally valid around a simulated reference trajectory. Such a model maps small deviations $\delta\mathbf{x}_0$ of an initial continuous state $\mathbf{x}_0^*$ to the corresponding deviations $\delta\mathbf{x}_s$ of a reference state $\mathbf{x}_s^*$ that lies on a switching threshold which is defined by the zero-level set of a switching function h (see Fig. 5). The linear approximation is computed by (Parker and Chua, 1989):

$$\delta\mathbf{x}_s = \underbrace{\left[I - \frac{\mathbf{f}(\mathbf{x}_s^*) \cdot \frac{\partial h}{\partial \mathbf{x}}(\mathbf{x}_s^*)}{\frac{\partial h}{\partial \mathbf{x}}(\mathbf{x}_s^*) \cdot \mathbf{f}(\mathbf{x}_s^*)} \right]}_{(1)} \underbrace{\mathbf{S}\,(t_s^*)}_{(2)} \delta\mathbf{x}_0 \tag{15}$$

Here, $\mathbf{f}(\mathbf{x}_s^*)$ is the evaluation of the dynamic equations at $\mathbf{x}_s^*$, $\frac{\partial h}{\partial \mathbf{x}}(\mathbf{x}_s^*)$ is the gradient of h evaluated at $\mathbf{x}_s^*$, and $\mathbf{S}\,(t_s^*)$ is the solution of Eq. 14 at t_s^* with $\mathbf{S}(t_0^*) = \mathbf{I}$. Term (2) of Eq. 15 maps the evolution of the initial deviation $\delta\mathbf{x}_0$ along the reference trajectory while the term (1) projects the resulting state along $\mathbf{f}$ onto the zero-level set of h.

Fig. 6 depicts how this mapping is adapted for each display case i. Under the assumption that the air temperature $T_{air,i}$ exhibits periodic behavior after the first period for constant disturbances and for unchanged $t_{v,i}$, the remainder of the time evolution of $T_{air,i}$ after $t_{s,i}^*$ can be neglected for control purposes. The state and sensitivity trajectories that are needed for the approximation of the embedded maps are computed simultaneously by the simulation of the hybrid model. Since the display cases are assumed to be independent, the sensitivity equations are evaluated separately for each display case which drastically reduces the number of sensitivities that must be computed.

The main idea is to formulate the resulting linear model of the controlled system as an algebraic optimization problem in which the finite-state embedded maps of the display cases appear as linear constraints [3]. Depending on the type of the cost function that is chosen, the overall problem can then be stated as a linear, a quadratic, or even a nonlinear programming problem. The control goal for the supermarket system is to desynchronize the air temperatures which corresponds to a uniform temporal distribution of the "time points of impact" $t^*_{s,i}$ of the air temperatures on the switching threshold δ_s. Thus, we are only interested in how a deviation $\delta t_{0,i}$ of the nominal valve closing time $t^*_{0,i}$ changes the next "time point of impact" $t^*_{s,i}$ of the air temperature $T_{air,i}$ on the switching threshold δ_s. Hence, a mapping $\delta t_{s,i} = H \cdot \delta t_{0,i}$ must be derived.

For simplicity, a new state vector $\mathbf{x}_{em,i} = [\mathbf{x}_{dc,i}, t]$ is defined for each display case that includes the time as an additional state. Since the switching function $h_i = T_{air,i} - \delta_s$ represents a constant switching threshold for each display case, its gradient is given by $\partial h_i / \partial \mathbf{x_{em,i}} = [0, 0, 1, 0, 0]$. Substituting this equation into Eq. 15, evaluating the right-hand side (with $\mathbf{f} = \mathbf{f_{i,vc}}$, see Eq. 3), and considering only the last row of the resulting matrix yields

$$\delta\ t_{s,i} = -\frac{1}{\frac{dT_{air,i}}{dt}(t^*_{s,i})} \cdot \mathbf{s}(t^*_{s,i}) \cdot \delta \mathbf{x}_{0,i} \qquad (16)$$

with

$$\mathbf{s}(t^*_{s,i}) = \begin{bmatrix} s_{T_{air,i},T_{g,i}}(t^*_{s,i}) \\ s_{T_{air,i},T_{w,i}}(t^*_{s,i}) \\ s_{T_{air,i},T_{air,i}}(t^*_{s,i}) \\ s_{T_{air,i},m_{ref,i}}(t^*_{s,i}) \\ -1 \end{bmatrix}^T \qquad (17)$$

In this equation, $s_{x_1,x_2}(t^*_{s,i})$ corresponds to the solution of the sensitivity equation at time $t^*_{s,i}$ that represents the effect of a change of x_2 on x_1. The final step is to express $\delta \mathbf{x}_{0,i}$ in terms of $\delta t_{0,i}$ which is achieved by linear interpolation: in addition to the simulation that is performed to determine the reference trajectory, a second simulation for the maximally allowed variation $\delta t_{0,i,max}$ from $t^*_{0,i}$ yields the maximal deviation of the state variables $\delta \mathbf{x}_{0,i,max}$. Here, $\delta t_{0,i,max}$ is a constant design parameter that is determined a priori by simulation such that the error of the linear approximation is negligible. Now, $\delta \mathbf{x}_{0,i}$ can be related linearly to $\delta t_{0,i}$ by $\delta\ \mathbf{x}_{0,i} = \frac{\delta \mathbf{x}_{0,i,max}}{\delta t_{0,i,max}} \cdot \delta\ t_{0,i}$. To ensure that the air temperatures do not violate the lower temperature bounds $\underline{T}_{air,i}$, additional linear constraints are derived that represent the variation $\delta T_{air,i,min}$ of the minimal air temperature $T_{air,i,min}$ of the reference trajectory with a variation of $t^*_{0,i}$ (see Fig. 6).

Since the embedded maps are only valid in a neighborhood $\epsilon := [\delta t^*_{0,i} - \delta t_{0,i,max}, \delta t^*_{0,i} + \delta t_{0,i,max}]$ around the reference trajectory, an algorithm is used that iterates between the generation of reference trajectories and optimization until convergence to the optimal solution is achieved. In each iteration j, the following steps are performed:

[3] Note that for the supermarket system, the optimal solution can be computed analytically from the embedded maps, as is described below. For other systems, however, optimization may be necessary.

(1) **Determination of the impact order:** A reference trajectory and the order of the impact points $t^*_{s,i}$ are determined by simulation with the optimal values $t^*_{0,j-1}$ from the previous iteration. This order remains fixed in iteration j.
(2) **Computation of optimal impact points:** The air temperature of the display case with the earliest impact point $t^*_{s,\bullet}$ is driven to the lower bound $T_{air,i,min}$ using the linear approximations. Considering the resulting time trajectory over two periods yields lower (impact time point after the first period) and upper (impact time point after the second period) reference values t_{min} and t_{max} for the impact time points of all other air temperatures. The optimal impact points $t^*_{s,i}$ for all other air temperatures are distributed equidistantly in the range $[t_{min}, t_{max}]$.
(3) **Computation of optimal parameters:** Since the optimal impact points are known for all air temperatures, the corresponding valve closing times $t^*_{0,i}$ are computed by inverting the embedded maps ($\delta t^*_{0,i} = H^{-1} \cdot \delta t^*_{s,i}$). If all $t^*_{0,i}$ are within ϵ, the algorithm **terminates** since the optimal values have been found. If one or more $t^*_{0,i}$ are outside ϵ, go to step (4).
(4) **Recomputation of the reference trajectory:** A new reference trajectory is computed using values for the valve opening times that are determined from the results of step (3). Here, all values that are outside the neighborhood ϵ are replaced by the upper (if they are larger than the maximum value in ϵ) or the lower (if they are smaller than the minimum value in ϵ) limits of ϵ. Then, the algorithm returns to step (3).

4. APPLICATION RESULTS

The optimization algorithm was implemented in *Matlab* and was tested with a large-scale supermarket refrigeration system with 10 display cases and 6 compressors. Fig. 7 shows the optimization results for a day-night scenario. From 0 to 7200 seconds, the system is in day-time operation, and after 7200 seconds, a night-time operation is assumed. During the day, the masses of the goods are varied to model the removal by customers and the replenishment by the supermarket staff, as shown in Fig. 7 (d). Tab. 1 shows the parameter values that were used in the simulation. The controller is capable of keeping all process variables within the bounds and desynchronizes the air temperatures very quickly, as is shown in the lower part of 7 (a). Furthermore, the low-level compressor controller detects the drastic change in the external disturbances at 7200 seconds and switches off four compressors to counteract the sudden change in the stationary compressor capacity. A comparison to previously obtained results for smaller systems shows that the control scheme significantly reduces the frequency of the compressor switching. As expected, the very major contribution to the run-time of the algorithm is the computational effort for the simulation of the nonlinear model. During nominal operation with only slowly varying disturbances, the algorithm only needs to execute very few simulations since the valve opening times are already close to the optimal values. Thus, an MPC iteration only takes a few seconds in this case. In the worst case, i.e. when the temperatures are completely synchronized, the computation time to achieve a complete desynchronization was less than 100 seconds on a standard PC. With some optimization of the prototype implementation, it seems realistic to achieve worst-case computation times in the region of 20 seconds.

Table 1. Parameter values used in the simulation studies.

n_{dc}	n_c	δ_s
10	6	4.6 °C °C
t_p	$\underline{T}_{air,1}$ - $\underline{T}_{air,10}$	$\overline{T}_{air,1}$ - $\overline{T}_{air,10}$
100 s	2 °C	5 °C
$t_{0,i,max}$	$\underline{P}_{suc}$	$\overline{P}_{suc}$ (day/night)
1 s	1 bar	1.7 bar / 1.9 bar
$\dot{Q}_{airload}$ (day)	$\dot{Q}_{airload}$ (night)	
3000 W	1800 W	
$\dot{m}_{ref-const}$ (day)	$\dot{m}_{ref-const}$ (night)	
0.2 $\frac{kg}{s}$	0.0 $\frac{kg}{s}$	

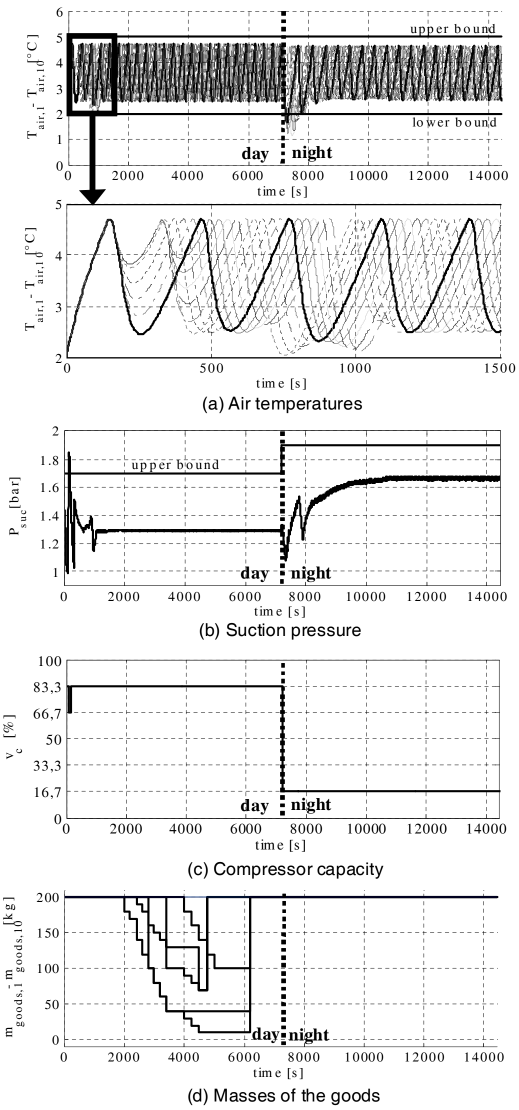

Fig. 7. Simulation results for a supermarket refrigeration system with 10 display cases and 6 compressors.

5. CONCLUSIONS

In this paper, a new hierarchical approach for the real-time capable control of large-scale supermarket refrigeration systems with hybrid dynamics is presented. Simple low-level temperature controllers are employed, and the high-level control task is the optimal adjustment of the parameters of these controllers to achieve a desynchronization of the air temperatures in the display cases which reduces the wear of the process equipment. Efficient desynchronizing control is achieved using a combination of model decomposition and approximation of the system dynamics by simple algebraic models. The main advantages of this approach over existing control techniques for supermarket refrigeration systems are that (a) the system is not linearized a priori. Any nonlinear characteristics of the system that are encoded in the reference trajectories are considered implicitly in the high-level control scheme, and (b) the computational performance is improved considerably since the original mixed-integer nonlinear dynamic optimization problem is replaced by a sequence of low-dimensional analytic problems that can be solved efficiently. Future work will concentrate on the extension of the developed technique to more general hybrid systems.

REFERENCES

Bemporad, A. and Morari, M. (1999). Control of systems integrating logic, dynamics, and constraints. *Automatica*, 35, 407–427.

Dankowicz, H. and Piiroinen, P.T. (2002). Exploiting discontinuities for stabilization of recurrent motions. *Dynamical Systems*, 17(4), 317–342.

Larsen, L.F.S., Geyer, T., and Morari, M. (2005). Hybrid MPC in supermarket refrigeration systems. In *Proc. 16th IFAC World Congress*. Th-E12-TO/5.

Larsen, L.F.S., Zamanabadi, R.I., Wisniewski, R., and Sonntag, C. (2007). Supermarket refrigeration systems - a benchmark for the optimal control of hybrid systems. Technical report for the Network of Excellence HYCON. Http://tinyurl.com/23nrkc.

Matveev, A.S. and Savkin, A.V. (2000). *Qualitative Theory of Hybrid Dynamical System*. Birkhäuser.

Parker, T.S. and Chua, L.O. (1989). *Practical Numerical Algorithms for Chaotic Systems*. Springer.

Sarabia, D., Capraro, F., Larsen, L.F.S., and De Prada, C. (2009). Hybrid NMPC of supermarket display cases. *Control Engineering Practice*, 17(4), 428–441.

Schild, A. and Lunze, J. (2008). Switching surface design for periodically operated discretely controlled continuous systems. In *Hybrid Systems: Computation and Control*, volume 4981 of *LNCS*, 471–485.

Sonntag, C., Devanathan, A., and Engell, S. (2008). Hybrid NMPC of a supermarket refrigeration system using sequential optimization. In *Proc. 17th IFAC World Congress*, 13901–13906.

Sonntag, C., Devanathan, A., Engell, S., and Stursberg, O. (2007). Hybrid nonlinear model-predictive control of a supermarket refrigeration system. In *Proc. IEEE Multi-Conference on Systems and Control (MSC/CCA)*, 1432–1437.

Wisniewski, R. and Larsen, L.F.S. (2008). Method for analysis of synchronization applied to supermarket refrigeration system. In *Proc. 17th IFAC World Congress*, 3665–3670.